JAMA Ophthalmology | Original Investigation

Characterization of Retinal Microvascular and Choroidal Structural Changes in Parkinson Disease

Cason B. Robbins, BS; Atalie C. Thompson, MD, MPH; Paramjit K. Bhullar, MD; Hui Yan Koo, BSc; Rupesh Agrawal, MMed; Srinath Soundararajan, BS; Stephen P. Yoon, MD; Bryce W. Polascik, BS; Burton L. Scott, MD, PhD; Dilraj S. Grewal, MD; Sharon Fekrat, MD

IMPORTANCE Noninvasive retinal imaging may detect structural changes associated with Parkinson disease (PD) and may represent a novel biomarker for disease detection.

OBJECTIVE To characterize alterations in the structure and microvasculature of the retina and choroid in eyes of individuals with PD and compare them with eyes of age- and sex-matched cognitively healthy control individuals using optical coherence tomography (OCT) and OCT angiography (OCTA).

DESIGN, SETTING, AND PARTICIPANTS This cross-sectional study was conducted at the Duke Neurological Disorders Clinic in Durham, North Carolina. Individuals aged 50 years or older with a diagnosis of PD were eligible for inclusion and underwent an evaluation and diagnosis confirmation before enrollment. Control individuals aged 50 years or older and without subjective cognitive dysfunction, a history of tremor, or evidence of motor dysfunction consistent with parkinsonism were solicited from the clinic or the Duke Alzheimer's Disease Prevention Registry. Individuals with diabetes, glaucoma, retinal pathology, other dementias, and corrected Early Treatment Diabetic Retinopathy Study (ETDRS) visual acuity worse than 20/40 Snellen were excluded. Data were analyzed between January 1, 2020, and March 30, 2020.

EXPOSURES All participants underwent OCT and OCTA imaging.

MAIN OUTCOMES AND MEASURES Generalized estimating equation analysis was used to characterize the association between imaging parameters and PD diagnosis. Superficial capillary plexus vessel density (VD) and perfusion density (PFD) were assessed within the ETDRS 6 × 6-mm circle, 6 × 6-mm inner ring, and 6 × 6-mm outer ring, as was the foveal avascular zone area. Peripapillary retinal nerve fiber layer thickness, macular ganglion cell–inner plexiform layer thickness, central subfield thickness, subfoveal choroidal thickness, total choroidal area, luminal area, and choroidal vascularity index (CVI) were measured.

RESULTS A total of 124 eyes of 69 participants with PD (39 men [56.5%]; mean [SD] age, 71.7 [7.0] years) and 248 eyes of 137 control participants (77 men [56.2%]; mean [SD] age, 70.9 [6.7] years) were analyzed. In the 6 × 6-mm ETDRS circle, VD (β coefficient = 0.37; 95% CI, 0.04-0.71; P = .03) and PFD (β coefficient = 0.009; 95% CI, 0.0003-0.018; P = .04) were lower in eyes of participants with PD. In the inner ring of the 6 × 6-mm ETDRS circle, VD (β coefficient = 0.61; 95% CI, 0.20-1.02; P = .003) and PFD (β coefficient = 0.015; 95% CI, 0.005-0.026; P = .004) were lower in eyes of participants with PD. Total choroidal area (β coefficient = −1.74 pixels^2; 95% CI, −3.12 to −0.37 pixels^2; P = .01) and luminal area (β coefficient = −1.02 pixels^2; 95% CI, −1.86 to −0.18 pixels^2; P = .02) were greater, but CVI was lower (β coefficient = 0.5%; 95% CI, 0.2%-0.8%; P < .001) in eyes of individuals with PD.

CONCLUSIONS AND RELEVANCE This study found that individuals with PD had decreased retinal VD and PFD as well as choroidal structural changes compared with age- and sex-matched control participants. Given the observed population differences in these noninvasive retinal biomarkers, further research into their clinical utility in PD is needed.

Invited Commentary

Supplemental content

Author Affiliations: Department of Ophthalmology, Duke University School of Medicine, Durham, North Carolina (Robbins, Thompson, Bhullar, Soundararajan, Yoon, Grewal, Fekrat); National Healthcare Group Eye Institute, Tan Tock Seng Hospital, Singapore, Singapore (Koo, Agrawal); Duke University, Durham, North Carolina (Polascik); Department of Neurology, Duke University School of Medicine, Durham, North Carolina (Scott).

Corresponding Author: Dilraj S. Grewal, MD, Department of Ophthalmology, Duke University School of Medicine, 2351 Erwin Rd, Durham, NC 27710 (dilraj.grewal@duke.edu).

JAMA Ophthalmol. doi:10.1001/jamaophthalmol.2020.5730
Published online December 23, 2020.

Parkinson disease (PD) is a progressive neurodegenerative condition that involves prominent motor dysfunction and nonmotor symptoms consistent with the loss of dopaminergic neurons in the substantia nigra that is attributed to the pathological accumulation of α-synuclein within cells.[1-3] The global impact of PD is increasing as the population ages, with its prevalence more than doubling from 1990 (2.5 million cases) to 2016 (6.1 million cases).[4]

The underlying cause of PD is not well understood. However, evidence has implicated cerebral small vessel disease as a potential risk factor for the development of PD, and PD has a higher prevalence of cerebral ischemic lesions.[5-7] On postmortem analysis of brain tissue from individuals with PD, Guan et al[5] observed decreased capillary branching as well as capillary fragmentation, shortening, and widening in multiple brain regions, including the substantia nigra. A prospective study showed an association between baseline small vessel disease and an increased 5-year risk of developing PD.[6]

No universally accepted biomarkers exist for the in vivo diagnosis of PD. Rather, the criterion standard for diagnosis is expert opinion in accordance with clinical guidelines released by the Movement Disorder Society.[8] In addition, the diagnosis of PD is complicated by its similarity to other parkinsonian conditions, including multiple system atrophy, progressive supranuclear palsy, and corticobasal degeneration.[9] Noninvasive tests to improve confidence in the diagnosis of PD remain a major unmet need.[10]

In the past decade, structural and functional changes in the retina have been studied as surrogate biomarkers for neurodegenerative changes in the brain.[11-13] In PD, patients often experience visual symptoms, including hallucinations, decreased contrast sensitivity, and impaired circadian rhythms.[3,14,15] Retinal ganglion cell dysfunction observed by electroretinography has been associated with PD disease severity.[16,17] In addition, on postmortem analysis, α-synuclein deposits have been observed in the retina in individuals with PD.[18] Thinning of the peripapillary retinal nerve fiber layer (RNFL) and ganglion cell-inner plexiform layer (GCIPL) on optical coherence tomography (OCT)[19] may discriminate individuals with PD from healthy control individuals.[20-23] Research on subfoveal choroidal thickness (SFCT) in PD has found conflicting results.[23,24] Choroidal vascularity index (CVI), a measure of the vascular status of the choroid that uses enhanced depth imaging (EDI) OCT, has not yet been assessed in individuals with PD.[25] Optical coherence tomography angiography (OCTA) may be able to detect retinal microvascular changes in individuals with PD.[26-29] Overall, previous research findings suggest that the retina may serve as a surrogate biomarker for cerebral vascular changes and global neurodegeneration in PD.[20,23]

In the present study, we used OCT and OCTA to characterize alterations in the structure and microvasculature of the retina and choroid in eyes of individuals with PD. We then compared the characterization with eyes of age- and sex-matched, cognitively healthy control individuals.

Key Points

Question Can noninvasive retinal imaging parameters from optical coherence tomography angiography and enhanced depth imaging optical coherence tomography serve as novel biomarkers for the diagnosis of Parkinson disease (PD)?

Findings In this cross-sectional study of eyes of 69 participants with PD and 137 healthy control participants, individuals with PD had decreased retinal vessel and perfusion densities, increased total choroidal area and choroid luminal area, and decreased choroidal vascularity index compared with age- and sex-matched control patients.

Meaning Results of this study suggest that noninvasive retinal imaging parameters warrant further investigation as potential biomarkers in PD.

Methods

This cross-sectional study was approved by the Duke Health Institutional Review Board, followed the tenets of the Declaration of Helsinki,[30] and complied with the Health Insurance Portability and Accountability Act of 1996. Written informed consent was obtained from all eligible individuals before enrollment. Control individuals were offered monetary compensation ($10) for study participation.

Study Participants

Individuals 50 years or older with a diagnosis of PD were recruited from the Duke Neurological Disorders Clinic in Durham, North Carolina. All individuals with PD were evaluated by an experienced movement disorders specialist among us (B.L.S.) prior to enrollment, and the clinical diagnosis of PD was confirmed in association with the International Parkinson and Movement Disorder Society clinical criteria.[8,31] Control participants were healthy volunteers 50 years or older and without subjective cognitive dysfunction, a history of tremor, or evidence of motor dysfunction consistent with parkinsonism. Control individuals were solicited from the Duke Neurological Disorders Clinic or the Duke Alzheimer's Disease Prevention Registry of cognitively healthy, community-dwelling volunteers with a Montreal Cognitive Assessment score of 23 or higher.

Exclusion criteria for all eligible individuals included a history of diabetes, glaucoma, retinal pathology, other dementias, and corrected Early Treatment Diabetic Retinopathy Study (ETDRS) visual acuity worse than 20/40 Snellen as measured by study staff at the time of image acquisition.

All study participants underwent cognitive evaluation using the Mini-Mental State Examination (MMSE; score range: 0-30, with higher scores indicating better performance) at the time of image acquisition. Years of education were assessed for each patient from the first grade onward.

OCTA Image Acquisition

All participants underwent imaging with the Zeiss Cirrus HD-5000 Spectral-Domain OCT with AngioPlex OCTA software,

Figure. Representative Optical Coherence Tomography Angiography (OCTA) Scan of the Right Eye of a Study Participant

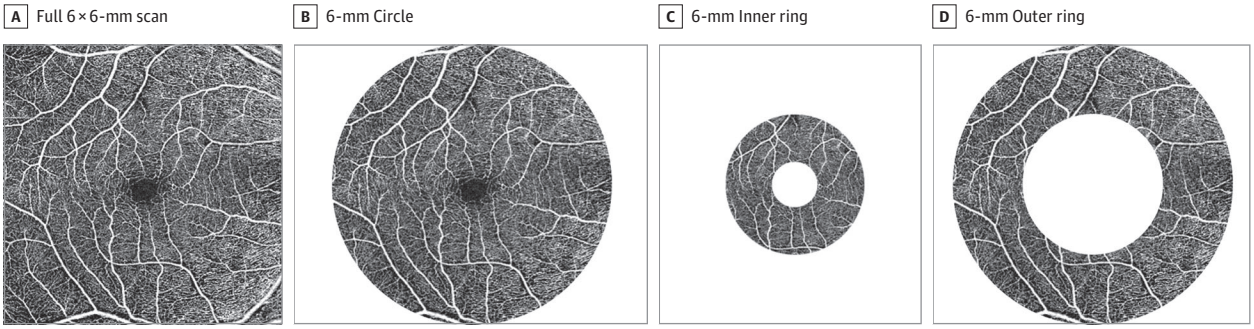

Vessel density and perfusion density were highlighted over these 4 regions of interest (A-D) in OCTA analysis, and the results are reported separately for each region.

version 11.0.0.29946 (Carl Zeiss Meditec), which uses an optical microangiography algorithm for analysis, has a scan rate of 68 000 A-scans per second, and uses eye tracking to reduce motion artifact.[32] The OCTA parameters were assessed using 6 × 6-mm OCTA images centered on the fovea. Images were manually assessed by trained study staff, and images with poor scan quality (less than 7/10 signal strength index), motion artifact, segmentation artifact, or focal signal loss were excluded.

Using the Zeiss AngioPlex software, version 11.0.0.29946, a thresholding algorithm was applied to OCTA en face images to create a binary skeletonized slab. Full-thickness retinal scans were segmented into the superficial capillary plexus, defined as the vasculature between the inner boundary of the internal limiting membrane and the outer boundary of the inner plexiform layer. The software detected the internal limiting membrane and calculated the inner plexiform layer as 70% of the distance from the internal limiting membrane to the estimated boundary of the outer plexiform layer, which was estimated to be 110 µm above the retinal pigment epithelium boundary.[33] The foveal avascular zone boundaries were automatically calculated by the software and then manually reviewed to correct inaccurate boundaries or exclude those that could not be corrected. We used 3 × 3-mm OCTA scans to assess the foveal avascular zone.

The vessel density (VD) and perfusion density (PFD) were measured in an ETDRS grid overlay. Vessel density was defined as the total length of perfused vasculature per unit area in the region of measurement. Perfusion density was defined as a percentage of area of perfused vasculature per unit area in a region of measurement. Both VD and PFD were measured over the 6 × 6-mm ETDRS circle and the inner and outer rings (**Figure**).

OCT Image Acquisition

A 512 × 128-µm macular cube, a 200 × 200-µm optic disc cube, and a high-definition, 21-line EDI foveal scan were acquired for each participant. Images with low signal strength (less than 7/10), motion artifact, segmentation artifact, or focal signal loss were excluded. Mean RNFL thickness (in micrometers) was measured over a 3.46-mm diameter circle centered on the optic disc. Mean GCIPL thickness (in micrometers) was quantified over the 14.13-mm^2 elliptical annulus area centered on the fovea. Central subfield thickness (CST [in micrometers]) was quantified as the thickness between the inner limiting membrane and retinal pigment epithelium at the fovea. The SFCT (in micrometers) was assessed as a linear measurement from the hyperreflective line of the outer border of the retinal pigment epithelium perpendicularly to the hyperreflective sclerochoroidal junction on the EDI foveal scan. The CVI, total choroidal area, and luminal area were calculated by applying image binarization techniques to EDI foveal scans using the protocol previously described by Agrawal et al.[25]

In brief, image binarization was performed with public domain software ImageJ, version 1.52r 26 (National Institutes of Health). A polygon tool was used to select the total choroidal area, which was added in the region-of-interest manager. After converting the image into an 8-bit image, we subsequently applied Niblack auto local thresholding, which gave the mean pixel value with SD for all of the points. On the EDI foveal scan, the luminal area was highlighted by applying the color threshold. To establish the luminal area within the selected polygon, we selected both the areas in the region-of-interest manager and merged by "AND" operation of ImageJ. The composite third area was added to the region-of-interest manager. The first area represents the total of the choroid selected, and the third composite area represents the luminal area. The CVI was calculated by dividing the luminal area by the total choroidal area.

Statistical Analysis

Each eye of a participant with PD was compared with 2 eyes of an age- and sex-matched control participant. Age-matched participants were chosen within 5 years of age of participants with PD. Patient demographic variables were compared at the participant level across groups using the χ^2 test for categorical variables and a 2-tailed, unpaired *t* test for continuous variables. The OCTA and OCT parameters were compared between participants with PD and control participants using generalized estimating equation (GEE) analysis with an exchangeable correlation structure to account for the inclusion of 2 eyes from the same participant. Area under the receiver

Table 1. Demographic Data for Study Participants

Variable	Mean (SD)	
	Participants with PD (n = 69)	Healthy control participants (n = 137)
Age, y	71.7 (7.0)	70.9 (6.7)
Female sex, No. (%)	30/69 (43.5)	60/137 (43.8)
Years of education	16.7 (3.0)	17.2 (2.3)
MMSE score	28.4 (2.4)	29.0 (2.8)

Abbreviations: MMSE, Mini-Mental State Examination; PD, Parkinson disease.

operating characteristic (AUROC) values were ascertained for each parameter using logistic regression with the diagnosis of PD as the outcome variable. The CVI was analyzed as a proportion (ie, number between 0 and 1) and reported as a percentage. β Coefficients for CVI are thus reported as percentages (ie, multiplied by 100). All *P* values were based on 2-tailed testing, and *P* = .05 was considered statistically significant; this value was not adjusted for multiple comparisons. Conclusions were based on observed differences in population means.

All statistical analyses were completed using SAS, version 9.4 (SAS Institute Inc). Data were analyzed between January 1, 2020, and March 30, 2020.

Results

We analyzed 124 eyes of 69 participants with PD (30 women [43.5%] and 39 men [56.5%]; mean [SD] age, 71.7 [7.0] years) and 248 eyes of 137 control participants (60 women [43.8%] and 77 men [56.2%]; mean [SD] age, 70.9 [6.7] years). A total of 14 eyes of participants with PD and 30 eyes of control participants were excluded according to the exclusion criteria (eg, image artifact, ETDRS visual acuity less than 20/40). **Table 1** describes the demographic and clinical characteristics of enrolled participants. Individuals with PD were well matched to their healthy control counterparts in terms of mean (SD) age, sex, MMSE score (28.4 [2.4] vs 29.0 [2.8]), and years of education (16.7 [3.0] years vs 17.2 [2.3] years).

Results of a GEE analysis of the association between OCTA parameters and PD diagnosis are shown in **Table 2**. Individuals with PD had lower superficial capillary plexus VD (β coefficient = 0.37; 95% CI, 0.04-0.71; *P* = .03) and PFD (β coefficient = 0.009; 95% CI, 0.0003-0.018; *P* = .04) in the 6 × 6-mm ETDRS circle. They also had lower superficial capillary plexus VD (β coefficient = 0.61; 95% CI, 0.20-1.02; *P* = .003) and PFD (β coefficient = 0.015; 95% CI, 0.005-0.026; *P* = .004) in the inner ring of the 6 × 6-mm ETDRS circle. The 2 patient groups did not differ with respect to the foveal avascular zone area (β coefficient = 0.016; 95% CI, −0.013 to 0.044; *P* = .29).

Results of a GEE analysis of the association of OCT and choroidal structural parameters with PD diagnosis are shown in **Table 3**. Individuals with PD did not differ from control patients in terms of CST (β coefficient = 2.95 µm; 95% CI, −3.97 to 9.87 µm; *P* = .40), mean GCIPL thickness (β coefficient = 0.62 µm; 95% CI, −1.74 to 2.99 µm; *P* = .61), or mean RNFL thickness (β coefficient = −0.21 µm; 95% CI, −2.79 to 2.37 µm; *P* = .87). The SFCT did not differ between groups; however, the total choroidal area (β coefficient = -1.74 pixels^2; 95% CI, −3.12 to −0.37 pixels^2; *P* = .01) and choroidal luminal area (β coefficient = -1.02 pixels^2; 95% CI, −1.86 to −0.18 pixels^2; *P* = .02) were larger but CVI was lower (β coefficient = 0.5%; 95% CI, 0.2%-0.8%; *P* < .001) in participants with PD. eFigure 1 in the Supplement demonstrates representative OCTA images and choroidal analysis of an individual with PD and an age- and sex-matched healthy control patient. Box plots with overlaid dot plots for each retinal parameter are shown in eFigure 2 in the Supplement.

Results of AUROC analysis for each parameter are detailed in separate columns in Table 2 and Table 3, and generated ROC curves for each parameter are shown in eFigure 3 in the Supplement. The AUROC values ranged from 0.50 to 0.63 as follows: GCIPL thickness, 0.50; SFCT, 0.50; RNFL thickness, 0.51; CST, 0.54; luminal area, 0.59; total choroidal area, 0.60; 6 × 6-mm inner ring VD and PFD, 0.63; and CVI, 0.63.

Discussion

In this cross-sectional study, we observed decreased retinal VD and PFD in the inner ring of the 6 × 6-mm ETDRS circle in individuals with an expert-confirmed diagnosis of PD compared with cognitively healthy control participants. On EDI-based analysis of the choroid, we observed increased choroidal area, increased choroidal luminal area, and decreased CVI in participants with PD compared with control participants. These differences suggest that objective retinal and choroidal structural changes may exist in individuals with a clinical diagnosis of PD. However, the AUROC analysis suggests that individual retinal parameters may not have sufficient discriminative capacity to function as independent biomarkers of disease with prespecified cutoff values that define disease presence or absence. However, when combined with clinical history and other existing tests, these choroidal and retinal microvascular imaging findings may hold the potential to improve clinician confidence in the diagnosis of PD.

The mechanism of retinal microvascular changes in PD is unclear. Individuals with PD have been noted to have increased cerebral small vessel disease compared with healthy control patients.[5-7] In addition, decreased retinal fractal dimension (associated with complexity of vascular branching) has been observed in individuals with cerebral small vessel disease[26] and, more recently, in individuals with PD.[28,29] Furthermore, the presence of α-synuclein, a pathophysiological factor in PD, in the retina of individuals with PD suggests that parkinsonian neurodegeneration occurs in the retina concomitantly with other brain structures, including the substantia nigra.[18] One may speculate that the retinal microvascular VD and PFD in individuals with PD may reflect the underlying neurodegenerative process with associated blood vessel regression.

In this large cross-sectional study, we did not observe differences in retinal structure (ie, CST, GCIPL thickness, or RNFL thickness) or SFCT between individuals with PD and healthy control individuals. Although α-synuclein is present in the retina in individuals with PD, it is not clear whether the neu-

Table 2. Generalized Estimating Equation Analysis of the Association of Optical Coherence Tomography Angiography Parameters With a Parkinson Disease Diagnosis

Variable	Participants with PD (n = 124)		Healthy control participants (n = 248)		β Coefficient (95% CI)	*P* value[a]	AUROC
	Mean (SD)	Median (range)	Mean (SD)	Median (range)			
6 × 6-mm Circle							
VD	17.34 (1.38)	17.70 (13.18 to 19.50)	17.69 (1.46)	18.08 (10.13 to 19.60)	0.37 (0.04 to 0.71)	.03	0.60
PFD	0.424 (0.035)	0.431 (0.314 to 0.483)	0.433 (0.040)	0.444 (0.182 to 0.479)	0.009 (0.0003 to 0.018)	.04	0.61
6 × 6-mm Inner ring							
VD	17.17 (1.74)	17.64 (11.00 to 19.90)	17.75 (1.68)	18.25 (10.25 to 20.00)	0.61 (0.20 to 1.02)	.003	0.63
PFD	0.412 (0.044)	0.421 (0.259 to 0.484)	0.426 (0.043)	0.439 (0.235 to 0.483)	0.015 (0.005 to 0.026)	.004	0.63
6 × 6-mm Outer ring							
VD	17.67 (1.32)	18.00 (13.74 to 19.79)	17.95 (1.48)	18.35 (10.41 to 19.90)	0.295 (−0.032 to 0.624)	.08	0.59
PFD	0.435 (0.034)	0.442 (0.332 to 0.488)	0.444 (0.038)	0.455 (0.240 to 0.488)	0.009 (0.0002 to 0.017)	.045	0.60
FAZ area[b]	0.215 (0.096)	0.210 (0.036 to 0.460)	0.229 (0.112)	0.215 (0.033 to 0.679)	0.016 (−0.013 to 0.044)	.29	0.52

Abbreviations: AUROC, area under the receiver operating characteristic curve; FAZ, foveal avascular zone; GEE, generalized estimating equation; OCTA, optical coherence tomography angiography; PD, Parkinson disease; PFD, perfusion density; VD, vessel density.

[a] *P* value was based on GEE analysis using an exchangeable correlation structure for the difference between means, accounting for the correlation between eyes of the same participant. Level of statistical significance was not adjusted for multiple comparisons.

[b] Measured using a 3 × 3-mm OCTA scan.

Table 3. Generalized Estimating Equation Analysis of the Association of Structural Optical Coherence Tomography Parameters and Choroidal Structural Parameters With a Parkinson Disease Diagnosis[a]

Variable	Participants with PD (n = 124)		Healthy control participants (n = 248)		β Coefficient (95% CI)	*P* value	AUROC
	Mean (SD)	Median (range)	Mean (SD)	Median (range)			
CST, μm	267.52 (24.28)	264.0 (207.0 to 361.0)	270.40 (26.55)	267.5 (197.0 to 389.0)	2.95 (−3.97 to 9.87)	.40	0.54
Mean GCIPL thickness, μm	75.10 (8.95)	75.0 (38.0 to 95.0)	75.52 (7.53)	76.0 (31.0 to 96.0)	0.62 (−1.74 to 2.99)	.61	0.50
Mean RNFL thickness, μm	88.77 (9.71)	89.0 (66.0 to 118.0)	88.38 (8.98)	89.0 (62.0 to 111.0)	−0.21 (−2.79 to 2.37)	.87	0.51
SFCT, μm	261.15 (87.66)	258.0 (64.0 to 453.0)	263.72 (91.42)	261.5 (66.0 to 600.0)	2.21 (−21.64 to 26.06)	.86	0.50
Total choroidal area, pixels^2	19.64 (4.68)	18.8 (8.7 to 31.8)	17.91 (5.44)	17.7 (7.5 to 39.1)	−1.74 (−3.12 to −0.37)	.01	0.60
Luminal area, pixels^2	12.35 (2.84)	11.9 (5.6 to 19.5)	11.34 (3.33)	11.3 (4.8 to 23.7)	−1.02 (−1.86 to −0.18)	.02	0.59
CVI, %	63.0 (0.90)	62.89 (61.12 to 65.42)	63.53 (1.20)	63.40 (60.57 to 68.56)	0.52 (0.24 to 0.79)	<.001	0.63

Abbreviations: AUROC, area under the receiver operating characteristic curve; CST, central subfield thickness; CVI, choroidal vascularity index; GCIPL, ganglion cell–inner plexiform layer; GEE, generalized estimating equation; PD, Parkinson disease; RNFL, retinal nerve fiber layer; SFCT, subfoveal choroidal thickness.

[a] GEE analysis adjusted for the correlation between 2 eyes of the same patient.

rodegenerative process would lead to a clinically detectable decrease in retinal thickness because of retinal ganglion cell loss. Subtle changes in the thickness of certain retinal layers and the choroid may be observed in specific individuals with PD and may be outside the limits of resolution of current imaging instrumentation. It has also been well documented that these alterations in RNFL, GCIPL, and CST are associated with normal aging, even beyond the sixth decade of life, and differ between male and female sexes.[34-36] After eliminating confounding from normal aging and sex differences by age- and sex-matching the study participants, we did not observe an association between a diagnosis of PD and these structural parameters. Previous studies have reported conflicting results on differences in RNFL and GCIPL thickness in PD even after age-matching the study participants with PD and control participants.[21-23] Long-term follow-up is needed to clarify if the rate of retinal structural change in individuals with PD is greater than what could be explained by normal aging.

Given the conflicting nature of previous reports on SFCT in individuals with PD,[23,24] we sought to further clarify choroidal structural changes in PD.[25] We observed no difference in SFCT, which was manually measured on EDI foveal scans. However, when assessing the total choroidal area, luminal area, and CVI using the whole scan and semiautomated image binarization, we observed differences between individuals with PD and control patients. This finding suggests that the choroidal vascularity may differ in individuals with PD without changes in choroidal thickness. The mechanism for these cho-

roidal changes is unclear but could be associated with the dysregulation of neurotransmitters, which control normal choroidal perfusion, including dopamine[37] and acetylcholine.[38,39] Further research characterizing choroidal changes across the clinical spectrum of PD and across a larger area of the retina may reveal the natural history of such changes.

Strengths and Limitations

This study has numerous strengths. We prospectively collated good-quality OCT and OCTA images from individuals with PD, and we were able to limit confounding associated with age and sex by matching these participants with cognitively healthy control individuals. We also used GEE analysis to account for the inclusion of 2 eyes from the same patient given that changes associated with a neurodegenerative disease may be expected to have implications for both eyes. In addition, we included an AUROC analysis, which demonstrated that, although the parameters exhibited mean population differences, they were individually unable to discriminate participants with PD from control participants. Perhaps a diagnostic index that incorporates multiple parameters may be better suited for distinguishing diagnoses. We recommend that future studies characterizing retinal imaging biomarkers for neurodegenerative disease include criteria and statistical analyses similar to those used in the present study given that many ocular, demographic, or imaging confounders could alter study results; results should be appropriately interpreted and reported.

This study has several limitations. Because there is no criterion standard biomarker for PD, we included individuals with an expert-confirmed clinical diagnosis of PD. However, it is possible that some individuals in this cohort had other parkinsonian disorders rather than true PD. In addition, because this is a cross-sectional study of individuals with varying degrees of PD severity, we were not able to identify the prognostic value of retinal imaging in PD. Long-term research is needed to clarify whether these imaging findings may be useful as biomarkers for the onset of PD or the development of more rapid deterioration from PD. OCTA imaging is particularly susceptible to motion artifact compared with other retinal imaging modalities. Images with poor quality or artifacts from tremor were excluded from the analysis, which restricted the pool of included participants to those with milder symptoms. Advances in OCTA technology and novel solutions for imaging in individuals with more advanced PD who have head tremors and other substantial motor symptoms will allow the assessment of retinal perfusion in individuals with the highest burden of neurodegeneration. In the statistical analysis that we conducted, we did not adjust the level of statistical significance for the presence of multiple comparisons because this adjustment may increase the rate of type II error. As such, findings in this study with $P < .05$ should be interpreted in context. We also were not able to evaluate the implication of commonly prevalent confounders, such as diabetes and glaucoma, for this cohort of patients with PD, which is necessary if these retinal and choroidal biomarkers are to be developed as screening tools.

Conclusions

In this cross-sectional study, a clinical diagnosis of PD was associated with decreased retinal microvascular perfusion and structural alterations in the choroid compared with findings in cognitively healthy control individuals. The findings of this study highlight the need for further research into retinal imaging as a potential novel biomarker for individuals with neurodegenerative diseases, such as PD. Future long-term studies that characterize the natural history of microvascular and structural retinal changes in individuals across the clinical spectrum of PD is warranted. Such studies may clarify whether these imaging findings may be useful as biomarkers for the onset of PD or the rapid deterioration from PD.

ARTICLE INFORMATION

Accepted for Publication: October 28, 2020.

Published Online: December 23, 2020. doi:10.1001/jamaophthalmol.2020.5730

Author Contributions: Mr Robbins and Dr Fekrat had full access to all of the data in the study and take responsibility for the integrity of the data and the accuracy of the data analysis. Drs Grewal and Fekrat shared senior authorship.
Concept and design: Robbins, Thompson, Grewal, Fekrat.
Acquisition, analysis, or interpretation of data: All authors.
Drafting of the manuscript: Robbins, Thompson, Bhullar, Koo, Grewal.
Critical revision of the manuscript for important intellectual content: Robbins, Thompson, Agrawal, Soundararajan, Yoon, Polascik, Scott, Grewal, Fekrat.
Statistical analysis: Robbins, Thompson.
Obtained funding: Grewal, Fekrat.
Administrative, technical, or material support: Robbins, Koo, Polascik, Grewal, Fekrat.
Supervision: Agrawal, Grewal, Fekrat.

Conflict of Interest Disclosures: Dr Scott reported receiving grants from the Biogen clinical trial, the Vaccinex clinical trial, the CHDI Foundation clinical trial, and the Neurocrine Biosciences clinical trial outside of the submitted study. No other disclosures were reported.

Meeting Presentations: Data from this study were presented in part at the 2019 Association for Research in Vision and Ophthalmology Annual Meeting; April 27-May 2, 2019; Vancouver, British Columbia, Canada. Data were presented in full at the virtual meetings of the 2020 Duke Trainee Day, June 5, 2020, and the 51st Annual Duke Medical Student Research Symposium, August 7, 2020, and the virtual meeting of the 2020 American Academy of Ophthalmology Annual Meeting; November 14-17, 2020.

Additional Contributions: Sandra Stinnett, PhD, Duke University, assisted with parts of the statistical analysis. She received no additional compensation, outside of her usual salary, for her contributions.

REFERENCES

1. Lotharius J, Brundin P. Pathogenesis of Parkinson's disease: dopamine, vesicles and alpha-synuclein. *Nat Rev Neurosci*. 2002;3(12):932-942. doi:10.1038/nrn983

2. de Lau LM, Breteler MM. Epidemiology of Parkinson's disease. *Lancet Neurol*. 2006;5(6):525-535. doi:10.1016/S1474-4422(06)70471-9

3. Chaudhuri KR, Healy DG, Schapira AH; National Institute for Clinical Excellence. Non-motor symptoms of Parkinson's disease: diagnosis and management. *Lancet Neurol*. 2006;5(3):235-245. doi:10.1016/S1474-4422(06)70373-8

4. GBD 2016 Parkinson's Disease Collaborators. Global, regional, and national burden of Parkinson's disease, 1990-2016: a systematic analysis for the Global Burden of Disease Study 2016. *Lancet Neurol*. 2018;17(11):939-953. doi:10.1016/S1474-4422(18)30295-3

5. Guan J, Pavlovic D, Dalkie N, et al. Vascular degeneration in Parkinson's disease. *Brain Pathol*. 2013;23(2):154-164. doi:10.1111/j.1750-3639.2012.00628.x

6. van der Holst HM, van Uden IWM, Tuladhar AM, et al. Cerebral small vessel disease and incident parkinsonism: The RUN DMC study. *Neurology*.

2015;85(18):1569-1577. doi:10.1212/WNL.0000000000002082

7. Song IU, Lee JE, Kwon DY, Park JH, Ma HI. Parkinson's disease might increase the risk of cerebral ischemic lesions. *Int J Med Sci*. 2017;14(4):319-322. doi:10.7150/ijms.18025

8. Postuma RB, Berg D, Stern M, et al. MDS clinical diagnostic criteria for Parkinson's disease. *Mov Disord*. 2015;30(12):1591-1601. doi:10.1002/mds.26424

9. Williams DR, Litvan I. Parkinsonian syndromes. *Continuum (Minneap Minn)*. 2013;19(5 Movement Disorders):1189-1212. doi:10.1212/01.CON.0000436152.24038.e0

10. Seifert KD, Wiener JI. The impact of DaTscan on the diagnosis and management of movement disorders: a retrospective study. *Am J Neurodegener Dis*. 2013;2(1):29-34.

11. London A, Benhar I, Schwartz M. The retina as a window to the brain—from eye research to CNS disorders. *Nat Rev Neurol*. 2013;9(1):44-53. doi:10.1038/nrneurol.2012.227

12. Jiang H, Delgado S, Liu C, et al. In vivo characterization of retinal microvascular network in multiple sclerosis. *Ophthalmology*. 2016;123(2):437-438. doi:10.1016/j.ophtha.2015.07.026

13. Yoon SP, Grewal DS, Thompson AC, et al. Retinal microvascular and neurodegenerative changes in Alzheimer's disease and mild cognitive impairment compared with control participants. *Ophthalmol Retina*. 2019;3(6):489-499. doi:10.1016/j.oret.2019.02.002

14. Ming W, Palidis DJ, Spering M, McKeown MJ. Visual contrast sensitivity in early-stage Parkinson's disease. *Invest Ophthalmol Vis Sci*. 2016;57(13):5696-5704. doi:10.1167/iovs.16-20025

15. La Morgia C, Ross-Cisneros FN, Sadun AA, Carelli V. Retinal ganglion cells and circadian rhythms in Alzheimer's disease, Parkinson's disease, and beyond. *Front Neurol*. 2017;8:162. doi:10.3389/fneur.2017.00162

16. Moschos MM, Tagaris G, Markopoulos I, et al. Morphologic changes and functional retinal impairment in patients with Parkinson disease without visual loss. *Eur J Ophthalmol*. 2011;21(1):24-29. doi:10.5301/EJO.2010.1318

17. Garcia-Martin E, Rodriguez-Mena D, Satue M, et al. Electrophysiology and optical coherence tomography to evaluate Parkinson disease severity. *Invest Ophthalmol Vis Sci*. 2014;55(2):696-705. doi:10.1167/iovs.13-13062

18. Ortuño-Lizarán I, Beach TG, Serrano GE, Walker DG, Adler CH, Cuenca N. Phosphorylated α-synuclein in the retina is a biomarker of Parkinson's disease pathology severity. *Mov Disord*. 2018;33(8):1315-1324. doi:10.1002/mds.27392

19. Huang D, Swanson EA, Lin CP, et al. Optical coherence tomography. *Science*. 1991;254(5035):1178-1181. doi:10.1126/science.1957169

20. Yu J-G, Feng Y-F, Xiang Y, et al. Retinal nerve fiber layer thickness changes in Parkinson disease: a meta-analysis. *PLoS One*. 2014;9(1):e85718. doi:10.1371/journal.pone.0085718

21. Garcia-Martin E, Satue M, Fuertes I, et al. Ability and reproducibility of Fourier-domain optical coherence tomography to detect retinal nerve fiber layer atrophy in Parkinson's disease. *Ophthalmology*. 2012;119(10):2161-2167. doi:10.1016/j.ophtha.2012.05.003

22. Satue M, Garcia-Martin E, Fuertes I, et al. Use of Fourier-domain OCT to detect retinal nerve fiber layer degeneration in Parkinson's disease patients. *Eye (Lond)*. 2013;27(4):507-514. doi:10.1038/eye.2013.4

23. Satue M, Obis J, Alarcia R, et al. Retinal and choroidal changes in patients with Parkinson's disease detected by swept-source optical coherence tomography. *Curr Eye Res*. 2018;43(1):109-115. doi:10.1080/02713683.2017.1370116

24. Eraslan M, Cerman E, Yildiz Balci S, et al. The choroid and lamina cribrosa is affected in patients with Parkinson's disease: enhanced depth imaging optical coherence tomography study. *Acta Ophthalmol*. 2016;94(1):e68-e75. doi:10.1111/aos.12809

25. Agrawal R, Gupta P, Tan KA, Cheung CM, Wong TY, Cheng CY. Choroidal vascularity index as a measure of vascular status of the choroid: measurements in healthy eyes from a population-based study. *Sci Rep*. 2016;6:21090. doi:10.1038/srep21090

26. McGrory S, Ballerini L, Doubal FN, et al. Retinal microvasculature and cerebral small vessel disease in the Lothian Birth Cohort 1936 and Mild Stroke Study. *Sci Rep*. 2019;9(1):6320. doi:10.1038/s41598-019-42534-x

27. Spaide RF, Klancnik JM Jr, Cooney MJ. Retinal vascular layers imaged by fluorescein angiography and optical coherence tomography angiography. *JAMA Ophthalmol*. 2015;133(1):45-50. doi:10.1001/jamaophthalmol.2014.3616

28. Kwapong WR, Ye H, Peng C, et al. Retinal microvascular impairment in the early stages of Parkinson's disease. *Invest Ophthalmol Vis Sci*. 2018;59(10):4115-4122. doi:10.1167/iovs.17-23230

29. Shi C, Chen Y, Kwapong WR, et al. Characterization by fractal dimension analysis of the retinal capillary network in Parkinson disease. *Retina*. 2020;40(8):1483-1491. doi:10.1097/IAE.0000000000002641

30. World Medical Association. World Medical Association Declaration of Helsinki: ethical principles for medical research involving human subjects. *JAMA*. 2013;310(20):2191-2194. doi:10.1001/jama.2013.281053

31. Postuma RB, Poewe W, Litvan I, et al. Validation of the MDS clinical diagnostic criteria for Parkinson's disease. *Mov Disord*. 2018;33(10):1601-1608. doi:10.1002/mds.27362

32. Rosenfeld PJ, Durbin MK, Roisman L, et al. ZEISS angioplex spectral domain optical coherence tomography angiography: technical aspects. *Dev Ophthalmol*. 2016;56:18-29. doi:10.1159/000442773

33. Iwasaki M, Inomata H. Relation between superficial capillaries and foveal structures in the human retina. *Invest Ophthalmol Vis Sci*. 1986;27(12):1698-1705.

34. Koh VT, Tham Y-C, Cheung CY, et al. Determinants of ganglion cell-inner plexiform layer thickness measured by high-definition optical coherence tomography. *Invest Ophthalmol Vis Sci*. 2012;53(9):5853-5859. doi:10.1167/iovs.12-10414

35. Altay L, Jahn C, Arikan Yorgun M, et al. Alteration of retinal layers in healthy subjects over 60 years of age until nonagenarians. *Clin Ophthalmol*. 2017;11:1499-1503. doi:10.2147/OPTH.S137223

36. Mauschitz MM, Holz FG, Finger RP, Breteler MMB. Determinants of macular layers and optic disc characteristics on SD-OCT: the Rhineland study. *Transl Vis Sci Technol*. 2019;8(3):34. doi:10.1167/tvst.8.3.34

37. Huemer KH, Zawinka C, Garhöfer G, et al. Effects of dopamine on retinal and choroidal blood flow parameters in humans. *Br J Ophthalmol*. 2007;91(9):1194-1198. doi:10.1136/bjo.2006.113399

38. Zhang Z, Zhou Y, Xie Z, et al. The effect of topical atropine on the choroidal thickness of healthy children. *Sci Rep*. 2016;6:34936. doi:10.1038/srep34936

39. Nickla DL, Wallman J. The multifunctional choroid. *Prog Retin Eye Res*. 2010;29(2):144-168. doi:10.1016/j.preteyeres.2009.12.002